

High pressure and high magnetic field studies of the electronic transport properties of the antiferromagnet $\text{Eu}_3\text{Ir}_4\text{Sn}_{13}$

L Mendonça-Ferreira¹, E M Bittar², I K E Bianchi¹, P F S Rosa^{3,4}, Z Fisk⁴, and P G Pagliuso³

¹Centro de Ciências Naturais e Humanas, UFABC, Santo André-SP, 09210-580, Brazil.

²Centro Brasileiro de Pesquisas Físicas, Rio de Janeiro-RJ, 22290-180, Brazil.

³Instituto de Física “Gleb Wataghin”, UNICAMP, Campinas-SP, 13083-859, Brazil.

⁴Department of Physics and Astronomy, University of California, Irvine, California 92697-4574, USA.

E-mail: leticie.ferreira@ufabc.edu.br

Abstract. In this work we report the effects of hydrostatic pressure and magnetic field on the electronic transport properties of the antiferromagnetic compound $\text{Eu}_3\text{Ir}_4\text{Sn}_{13}$ ($T_N \sim 10$ K). Single crystals of $\text{Eu}_3\text{Ir}_4\text{Sn}_{13}$ were synthesized using the Sn self-flux technique. DC electrical resistivity measurements as a function of temperature were performed by means of the four-probe technique. The high-temperature anomaly at $T^* \sim 57$ K attributed to a structural distortion of the $\text{Sn}_1\text{Sn}_{212}$ cages in $\text{Eu}_3\text{Ir}_4\text{Sn}_{13}$ is rapidly decreased to lower temperatures at a rate $dT^*/dP = 2$ K/kbar, while the antiferromagnetic transition due to the Eu^{2+} ions is only weakly affected. Our data do not indicate any magnetoelastic effect associated with the structural instability at T^* . Furthermore, the suppression of the lattice distortion by application of external pressure is not accompanied by the emergence of superconductivity, possibly due to strong magnetic correlations between the Eu^{2+} localized magnetic moments.

1. Introduction

The ternary stannides compounds $R_3M_4\text{Sn}_{13}$ (R = rare-earth or alkaline-earth, M = transition metal) [1] have recently regained interest due to the possible interplay between superconductivity and the occurrence of a structural quantum critical point, as claimed in $\text{Ca}_3\text{Ir}_4\text{Sn}_{13}$ ($T_c \sim 7$ K) and in $\text{Sr}_3\text{Ir}_4\text{Sn}_{13}$ ($T_c \sim 5$ K) [2]. A common feature to both compounds is the occurrence of distinct anomalies in the electrical resistivity at temperatures well above the superconducting transition related to a structural transition from a simple cubic structure to a superlattice variant. The superlattice transition temperature, T^* , can be suppressed to zero by combining chemical and/or external pressure, and is accompanied by an increase in the superconducting transition temperature, giving rise to a superconducting dome in the temperature-pressure phase diagram. Interestingly, the same behavior has been recently reported in $\text{La}_3\text{Co}_4\text{Sn}_{13}$ [3]. In this regard, these results motivate further systematic investigations of the superlattice quantum phase transition and its relationship with the occurrence of superconductivity and/or magnetism in other related materials.



A similar anomaly was observed in the electrical resistivity of the antiferromagnet $\text{Eu}_3\text{Ir}_4\text{Sn}_{13}$ ($T_N \sim 11$ K) [4]. The high temperature anomaly at $T^* \sim 50$ K was confirmed latter in the heat capacity data, although it has not been unambiguously discernible in the magnetic susceptibility [5]. X-ray resonant magnetic scattering (XRMS) has identified the anomaly at T^* as a crystallographic distortion due to a displacement of the Sn ions in the $\text{Sn}_1\text{Sn}_{12}$ polyhedron. According to XRMS and neutron diffraction experiments, both the structural distortion and the antiferromagnetic (AFM) ordering are characterized by the same propagation vector $\tau = \mathbf{q} = (\mathbf{0}, (\mathbf{1}/2), (\mathbf{1}/2))$ in the reciprocal space [6]. Our previous pressure dependent resistivity measurements on a $\text{Eu}_3\text{Ir}_4\text{Sn}_{13}$ single crystal up to 8 kbar have revealed that T^* is strongly pressure-dependent and decreases linearly with increasing pressure, while the magnetic ordering temperature T_N is weakly affected in the pressure range investigated [5].

In the present work we have extended our early study on $\text{Eu}_3\text{Ir}_4\text{Sn}_{13}$ to higher pressures ($P < 26$ kbar), and have also investigated the effects of magnetic field on the electronic transport properties of the intermetallic $\text{Eu}_3\text{Ir}_4\text{Sn}_{13}$. We discuss our pressure and magnetic field dependent data taking into account the possible coupling between the structural transition and the magnetic interactions in this compound and we also compare our findings with the properties of other $R_3M_4\text{Sn}_{13}$ family members.

2. Experimental details

Single crystals of $\text{Eu}_3\text{Ir}_4\text{Sn}_{13}$ were grown from the melt in Sn flux as described previously [7]. The structure and phase purity were examined by X-ray powder diffraction (XRD) at room temperature. The X-ray patterns confirmed that our single crystals are single-phased and crystallize in the cubic $\text{Yb}_3\text{Rh}_4\text{Sn}_{13}$ -type structure, space group $Pm-3n$, with lattice parameter equal to 7.78 Å [8]. Temperature dependent DC electrical resistivity measurements were carried out in a Physical Properties Measurement System (PPMS), with applied magnetic fields up to $H = 90$ kOe and external pressure up to $P = 26$ kbar, by means of the conventional four-contact configuration. Experiments under hydrostatic pressure were carried out in a clamp-type CuBe cell using silicon oil as the pressure transmitting medium. Pressure in the sample region was resistively determined from the pressure induced shift in the T_c of a small piece of Pb.

3. Results and Discussion

Figure 1 displays the temperature dependence of the electrical resistivity, $\rho(T)$, of our $\text{Eu}_3\text{Ir}_4\text{Sn}_{13}$ single crystal for different applied pressures. The main panel shows the temperature interval below 70 K, while the inset displays the $\rho(T)$ curves for some selected pressures from 300 K down to 2 K. The resistivity behavior of $\text{Eu}_3\text{Ir}_4\text{Sn}_{13}$ is metallic ($d\rho(T)/dT > 0$) over the whole temperature range investigated. However, we can distinguish different regimes and anomalies as the temperature decreases. From room- T down to the temperature T^* (see inset), the $\rho(T)$ curves show a negative curvature ($d^2\rho(T)/dT^2 < 0$). Below T^* , a hump-like feature is discernible in the electrical resistivity at zero applied pressure. With further cooling, $\rho(T)$ changes to a new regime with a linear-like decrease at a higher rate. This regime goes down to the temperature at which the magnetic order takes place, which manifests itself as a kink at $T_N \sim 10$ K. Within the magnetic phase, the electrical resistivity follows a power law behavior, as discussed below.

It is noteworthy that the anomaly at T^* is identical to the one seen in other ternary stannides compounds, such as the superconductors $\text{Ca}_3\text{Ir}_4\text{Sn}_{13}$ and $\text{Sr}_3\text{Ir}_4\text{Sn}_{13}$, for which T^* is equal to 33 K and 147 K, respectively [2]. Interestingly, recent reports have attributed the anomaly at T^* to a structural distortion of the $\text{Sn}_1\text{Sn}_{12}$ polyhedrons due to the displacements of the Sn ions in the cages [6]. Our results show that the application of hydrostatic pressure does not affect the qualitative high temperature behavior of the resistivity. As one can see from the inset of figure 1, $\rho(T)$ decreases as P increases, as usually occurs in metals. Nevertheless, application of pressure has a huge effect on the structural transition. The temperature T^* shifts

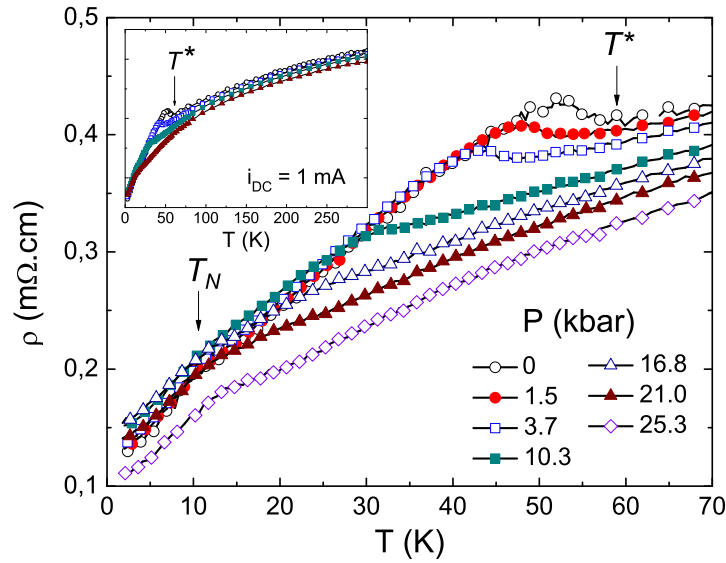


Figure 1. Temperature dependence of the electrical resistivity $\rho(T)$ of $\text{Eu}_3\text{Ir}_4\text{Sn}_{13}$ submitted to different hydrostatic pressures. Main panel: expanded view of $\rho(T)$ in the temperature range close to T^* and T_N . Inset: $\rho(T)$ from 300 K down to 2 K shown for selected pressures.

to lower temperatures and the hump-like feature initially observed at lower pressures evolves continuously to a kink upon increasing P . Remarkably, the application of low pressures has no significant effect on the electrical resistivity between $T^*(P)$ and T_N . As suggested in ref.[2] for superconducting $(\text{Ca}_{1-x}\text{Sr}_x)_3\text{Ir}_4\text{Sn}_{13}$, the linear temperature dependence of $\rho(T)$ may be attributed to the softening of optical phonon modes at T^* . The $\rho(T)$ data obtained for our $\text{Eu}_3\text{Ir}_4\text{Sn}_{13}$ single crystal in the T -range $T_N < T < T^*$ points to a non-trivial evolution of the soft modes with pressure.

Based on the data from figure 1, we constructed the temperature-pressure ($T - P$) phase diagram of $\text{Eu}_3\text{Ir}_4\text{Sn}_{13}$ by mapping T_N and the anomaly at T^* . The temperature T^* was considered as the temperature where $\rho(T)$ deviates from the high- T metallic behavior (indicated by the arrow in Fig. 1), and T_N corresponds to the kink observed at low temperatures. The ($T - P$) phase diagram is depicted in figure 2.

As it occurs in other compounds of the series [2], we see from figure 2 that the structural distortion at T^* is strongly suppressed by the application of pressure. The initial value decreases at a rate of 2 K/kbar and extrapolates to zero at a critical pressure $P_c = 27.5$ kbar. On the other hand, the Néel temperature is weakly affected by pressure, exhibiting a slight increase up to 8.3 kbar followed by a weak decrease at higher pressures. This confirms our previous results obtained under $P < 8$ kbar for a $\text{Eu}_3\text{Ir}_4\text{Sn}_{13}$ single crystal from the same batch than the one studied here [5]. Moreover, regarding the structural transition, our results are in very good agreement with data reported for superconducting $(\text{Ca}_{1-x}\text{Sr}_x)_3\text{Ir}_4\text{Sn}_{13}$ [2]. However, application of pressure does not induce superconductivity in $\text{Eu}_3\text{Ir}_4\text{Sn}_{13}$ and the AFM ordering remains stable up to the highest pressure of $P = 25.3$ kbar.

Concerning the magnetic phase below T_N , we have fitted the $\rho(T)$ curves to a power law T -dependence of the type $\rho(T) = \rho_0 + A.T^n$ where ρ_0 is the residual resistivity. According to our analysis, the resistivity for $T < T_N$ is described by a power law with exponent $n = 1.5(1)$ and a coefficient $A = 2.2(4).10^{-6}$ mΩ.cm/K. This non-Fermi-liquid-like behavior ($n \neq 2$) and the linear-like T -dependence of $\rho(T)$ for $T_N < T < T^*$ indicate that fluctuations of the structural

order parameter and magnetic excitations of the ordered state have non-trivial contributions to the electronic scattering at low- T for $\text{Eu}_3\text{Ir}_4\text{Sn}_{13}$. In addition, the analysis of the fitted parameters shows a pressure-dependent residual resistivity with an initial enhancement under pressure for $P < 8$ kbar, followed by a decrease at higher pressures, as depicted in figure 2 together with the $(T - P)$ phase diagram. As T_N is only weakly affected by pressure, this result suggests that the evolution of the fluctuations associated with the structural order parameter is most likely the responsible for the pressure dependence of ρ_0 .

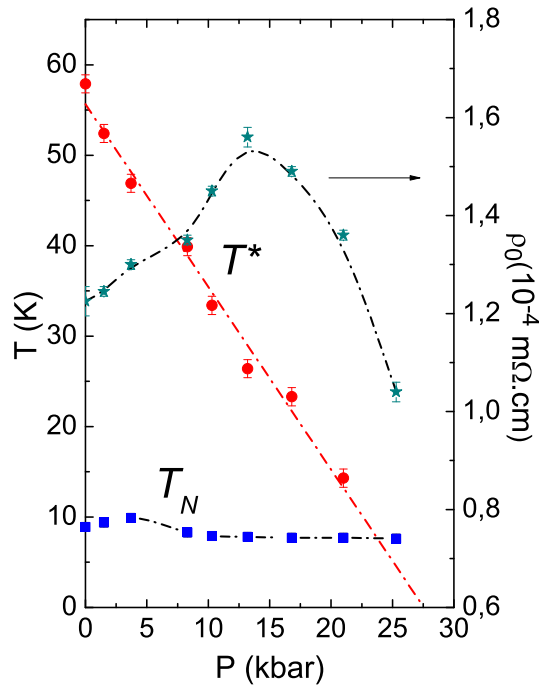


Figure 2. Temperature-pressure phase diagram for $\text{Eu}_3\text{Ir}_4\text{Sn}_{13}$ constructed from data shown in figure 1; T^* refers to the temperature where the structural distortion takes place, and T_N is the Néel temperature.

We now turn our attention to the analysis of the influence of applied magnetic fields on the electrical resistivity. Figure 3 shows the temperature dependence of the electrical resistivity of $\text{Eu}_3\text{Ir}_4\text{Sn}_{13}$ under various applied magnetic fields. The main panel presents the data in the temperature region below 85 K. The inset is an expanded view of the T -range around the magnetic transition. We first note that the metallic high temperature behavior is not affected by the magnetic field. Concerning the structural distortion, application of magnetic field does not change the hump-like feature in the curves, neither the shape, the position nor its intensity. Hence we do not observe any magnetoelastic effect associated with the structural distortion in our $\text{Eu}_3\text{Ir}_4\text{Sn}_{13}$ single crystal. Nevertheless, we notice that the applied magnetic field affects the ordered state of $\text{Eu}_3\text{Ir}_4\text{Sn}_{13}$ below T_N . As shown in Fig. 1, the transition to the AFM state under $H = 0$ manifests itself as a kink which separates the almost linear T -dependence of $\rho(T)$ at higher T from a power law behavior below T_N . As the applied magnetic field increases, a new feature develops within the ordered state. As we can see in the inset of figure 3, this feature evolves continuously as H increases. In order to build the temperature-magnetic field $(T - H)$ phase diagram, we adopted the criterion shown in figure 4 to define two characteristic temperatures. In figure 4 we present the resistivity curve and its corresponding derivative $d\rho(T)/dT$ for the T -range around the magnetic transition. Data taken under $H = 0$ and $H = 50$ kOe are presented in panels (a) and (b), respectively. The Néel temperature T_N is defined as the temperature corresponding to the maximum in $d\rho(T)/dT$ while a second

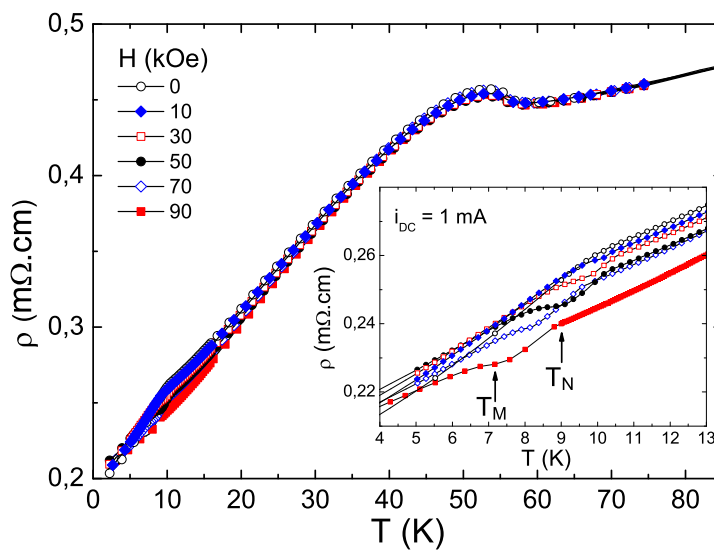


Figure 3. Temperature dependence of the electrical resistivity of $\text{Eu}_3\text{Ir}_4\text{Sn}_{13}$ under various applied magnetic fields. Inset: Expanded view of the $\rho(T)$ in the temperature range close to the magnetic transition.

temperature, denoted by T_M , corresponds to the minimum in the derivative curve. Adopting this criterion, we constructed the $(T - H)$ phase diagram displayed in figure 5.

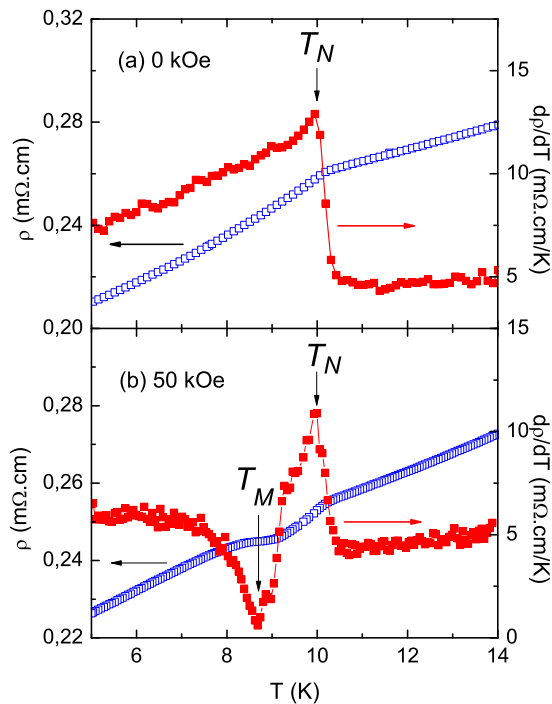


Figure 4. Details of the temperature dependence of the electrical resistivity $\rho(T)$ of $\text{Eu}_3\text{Ir}_4\text{Sn}_{13}$ and the corresponding derivative curve near the magnetic transition. The plots refer to data obtained under (a) 0 kOe and (b) 50 kOe.

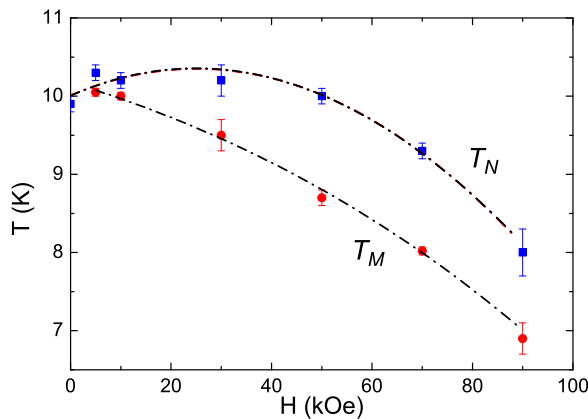


Figure 5. Temperature-magnetic field phase diagram for $\text{Eu}_3\text{Ir}_4\text{Sn}_{13}$ constructed from data shown in figure 3.

In view of our early results [5], we are inclined to correlate this structure with the step transition observed for $\text{Eu}_3\text{Ir}_4\text{Sn}_{13}$ in the magnetization data as a function of applied magnetic field. As reported in ref.[5], a metamagnetic transition occurs within the ordered state of $\text{Eu}_3\text{Ir}_4\text{Sn}_{13}$ when the field is oriented along the [100] axes, but is absent when H is rotated to the [110] direction. One could speculate that the field-induced structure in the low temperature $\rho(T)$ curves has the same origin as the metamagnetic transition previously seen in $\text{Eu}_3\text{Ir}_4\text{Sn}_{13}$. Additional experiments will be valuable to elucidate this issue. For instance, T -dependent specific heat measurements under magnetic field are in progress to confirm this scenario.

4. Conclusions

In summary, in this work we have investigated the effects of hydrostatic pressure and magnetic field on the electronic transport properties of the antiferromagnet $\text{Eu}_3\text{Ir}_4\text{Sn}_{13}$. As observed in other ternary stannides materials, the structural distortion is strongly suppressed to lower- T with increasing pressure, while the AFM transition is weakly affected. Despite the suppression of the structural transition, strong magnetic interactions persist up to the highest applied pressure, and superconductivity is not observed down to the lowest temperature achieved.

Acknowledgments

L. Mendonca-Ferreira thanks the financial support by FAPESP-SP under Grants Nos. 2014/07730-7 and 2011/19924-2. The authors acknowledge the support by FAPESP-SP (particularly Grants Nos. 2013/17427-7, 2013/20181-0, 2012/04870-7), FAPERJ-RJ (Grant No. 111.382/2013), CNPq-Brazil and AFOSR MURI.

References

- [1] Remeika J, Espinosa G, Cooper A, Barz H, Rowell J, McWhan D, Vandenberg J, Moncton D, Fisk Z, Woolf L, Hamaker H, Maple M, Shirane G and Thomlinson W 1980 *Solid State Commun.* **34** 923
- [2] Klintberg L E, Goh S K, Alireza P L, Saines P J, Tompsett D A, Logg P W, Yang J, Chen B, Yoshimura K and Grosche F M 2012 *Phys. Rev. Lett.* **109** 237008
- [3] Slebarski A, Fijakowski M, Maska M M, Mierzejewski M, White B D and Maple M B 2014 *Phys. Rev. B* **89** 125111
- [4] Sato H et al. 1993 *Physica* **186-188** 630
- [5] Mendonça-Ferreira L et al 2006 *Physica B* **384** 332
- [6] Mardegan J R L, Aliouane N, Coelho L N, Agüero O, Bittar E M, Lang J C, Pagliuso P G, Torriani I L and Giles C 2013 *IEEE Trans. Magn.* **49** 4652
- [7] Israel C et al 2005 *Physica B* **359-361** 251
- [8] Agüero O E 2007 *Estudo estrutural de sistemas nanoestruturados, compostos intermetálicos e cobaltitas*, Ph.D. thesis, University of Campinas, Brazil.